Digital Object Identifier (DOI): 10.1109/TIE.2016.2549503

IEEE Transactions on Industrial Electronics (Volume:63, Issue:8) August 2016

Thermal Stress Analysis and MPPT Optimization of Photovoltaic Systems

Markus Andresen
Giampaolo Buticchi
Marco Liserre

Suggested Citation

M. Andresen, G. Buticchi and M. Liserre, "Thermal Stress Analysis and MPPT Optimization of Photovoltaic Systems," in IEEE Transactions on Industrial Electronics, vol. 63, no. 8, pp. 4889-4898, Aug. 2016.

Thermal Stress Analysis and MPPT Optimization of Photovoltaic Systems

Markus Andresen, *Student Member, IEEE*, Giampaolo Buticchi, *Member, IEEE*, Marco Liserre, *Fellow, IEEE*

***Abstract*— In the last years, the optimization of the energy harvesting of photovoltaic systems during fast variable irradiance conditions has been an active area of research and of competition among the companies. The proposed fast MPPT (Maximum Power Point Tracking) algorithms can produce extremely variable loading of the power semiconductors resulting in a decrease of the system lifetime, which in consequence can nullify the economic advantage of higher energy harvesting. This work analyses the problem with a deep theoretical and laboratory work. Then a multi-objective MPPT, which limits the positive temperature gradient and the maximum junction temperature of the power semiconductors, is introduced and fully validated in the laboratory with a mission profile emulating variable irradiance conditions.**

***Index Terms*— Maximum power point tracking, Photovoltaic systems, Reliability, Thermal management, active thermal control**

I. Introduction

Photovoltaic power plants are built worldwide to increase the renewable energy production and power electronics are a key factor for their grid integration [1]. To amortize their high manufacturing costs, these systems need to harvest maximum power for lifetimes of 20 years. These goals, maximum energy and long life, which later on in the paper will be demonstrated as conflicting, had push tremendously the research towards more performing MPPT algorithms [2],[3] and more efficient and robust power electronics solutions [4]-[5]. The MPPT strategies offer different advantages with respect to tracking speed, complexity and performance under partial shading conditions. The maximization of the energy harvesting is important to justify the cost of a PV system. However, the possible failure of the power converter is also impacting the cost of PV energy. Among the most sensitive components to failure are the power semiconductors[6]. The underlying aging mechanism of the power semiconductors is thermal cycling, which causes mechanical stress between materials with different coefficients of thermal extension,[7],[8]. Several technologies have been proposed by companies which manufacture discrete components and modules to reduce the effect of thermal stress [9] but the associated larger costs discourage a wide use in a market which today is dominated by cost minimization [10].

A reduction of thermal cycling, by means of control, for the power semiconductors increases the reliability of the system [11] and would have no additional costs. In literature an analysis is done for the reliability critical parts of the photovoltaic system [6]. The reliability of several components, different Maximum Power Point Tracking (MPPT) algorithms and anti-island schemes is evaluated, but only in [12] an action is taken to improve the algorithms with respect to reliability. Of high importance for the reduction of thermal cycling is the knowledge about the junction temperature itself, because if affects the physical failure mechanisms within the module. The detection of the junction temperature itself is a challenging research objective, which either requires special measurement equipment or special software [13].

This work proposes to apply a "lifetime-optimized" MPPT to control the stress of the power electronics in the DC/DC converter. The thermal effects of traditional MPPT algorithms are analyzed and an algorithm is introduced, which reduces the thermal stress during fast changing irradiance and limits the maximum junction temperature.

In section II an introduction in reliability issues of power electronic modules is given, while section III analyses the problem of fast changing irradiance in combination with MPPT for the single and the double stage PV systems. Section IV describes the proposed modified MPPT algorithm and in section V the laboratory setup is presented together with tests of the steady state and the dynamical behavior of the algorithm. The experimental analysis of the tradeoff between lifetime consumption and maximum harvested energy is analyzed in section VI. The measurement or estimation of the junction temperature is discussed in section VII with experimental results.

II. Reliability in power electronics

Power electronics are often assembled in power electronic modules for improved heat transfer capability and for increased power density. In these modules, the chips are mounted on multi-layer configurations, called direct bonded copper (DBC), to ensure the electrical insulation and good heat dissipation. Thereby the chips are soldered on the DBC, which consists of a substrate enclosed by two separated layers of copper. Beside the low heat transfer capability of the substrate compared to copper, these materials have unequal coefficients of thermal extension (CTE). The resulting problem is the strain between the layers caused by temperature gradients and variations in the temperature. This strain is regarded as the main reason for aging

Manuscript received November 3, 2015; revised February 12, 2016 and March 13, 2016; accepted March 15, 2016.

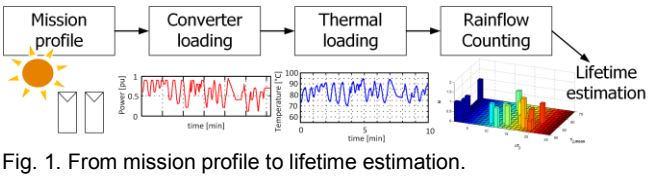

Fig. 1. From mission profile to lifetime estimation.

of power electronic modules in literature and has led to significant effort to overcome the reliability issues and to monitor the degradation [14]. Consequently, to increase the lifetime of the power semiconductors, either the interconnections between the different layers with CTE-mismatch have to be improved or the thermal cycles need to be reduced.

An estimation of the remaining lifetime requires the knowledge of the mission profile. In Fig. 1, the mandatory steps to obtain a power semiconductor's lifetime estimation in a PV application are shown. First, the mission profile is used to obtain the converter loading and the electrical and thermal properties are used to obtain the temperature profiles of the power semiconductors. Afterwards, Rainflow counting is applied to identify the thermal cycles in the profile and with a model provided by the manufacturer, the lifetime can be estimated. A possible lifetime model can be extracted by linear interpolation of the LESIT results [15], which were obtained by accelerated lifetime tests. This model is described with (1), whereby $T_{j,mean}$ defines the average temperature of a thermal cycle ΔT_j.

$$N_f = 4.48 \cdot 10^{14} \cdot (\Delta T_j)^{-5.024} \cdot e^{(-T_{j,mean}+77.5)\cdot 0.0555} \quad (1)$$

This lifetime model defines the number of thermal cycles to failure N_f for a singular magnitude. Since a real mission profile contains several thermal cycles with different magnitudes, the damage needs to be accumulated, which can be done with the Palmgren-Miners rule (2), where N_i is the lifetime for the stress range i and n_i is the actual number of applied stress range I (2). As $c \geq 1$, the device fails.

$$\sum_{i=1}^{k} \frac{n_i}{N_i} = c \quad (2)$$

This linear extrapolated lifetime model is known to lack of precision, but still it indicates the mathematical connection to the failure mechanisms, such as bond wire liftoff and solder fatigue. Despite the simple form of the lifetime model in (1), the exponential dependence of the thermal cycles is also shown in many lifetime models of failure mechanisms [16] presented in literature. To obtain the magnitude of the thermal cycles ΔT_j, Rainflow counting [17] is usually applied for the junction temperature profile.

III. Thermal Stress of Maximum Power Point Tracking

Photovoltaic power plants have challenged the engineers to reduce the ground leakage currents, achieve high energy conversion efficiency and to comply with international regulations. [18]. For cost efficiency of a PV power plant, the maximum energy from the array needs to be harvested. To extend the operation range, often a boost converter is used to step-up the voltage to the level of the DC link voltage. The structure of a single phase one and double-stage PV system is shown in Fig. 2. The MPPT of the two stages converter in this work is performed by control of the duty cycle d, which is expressed by the ratio of the turn on time of the IGBT ton and the sampling time T_s or with the PV array voltage U and the DC-link voltage U_{dc} as shown in (3). Contrary, the MPPT of the single stage PV converter is performed by current control of the converter.

$$d = \frac{t_{on}}{T_s} = 1 - \frac{U}{U_{dc}} \quad (3)$$

To perform MPPT, the controller needs to have information about the current operation point of the PV array and at least the current and voltage measurements of one additional operation point. To obtain the voltage and current measurement of the second set point, the actual operation point needs to be changed, which changes the losses of the system and thus causes thermal stress for the power electronics by means of a ΔT. The thermal swing depends on the MPPT algorithm, which normally implies the control of the current or the voltage of the PV array. Thereby, the thermal swing caused by the perturb and observe algorithms are expected to be low, while the measurement of the short circuit current or the open circuit voltage are expected

TABLE I
SIMULATION PARAMETERS.

Variable	*grid frequency f_s*	*Grid voltage*	*C_f*	*L_{fg}*	*L_{fc}*	*Irradiation*	*U_{dc}*	*U_{OC}*	*I_{SC}*
Value single stage PV power plant	50 Hz	230 V rms	2.2 µF	1 mH	6.9 mH	1 kW/m²	variable	552 V	12,75 A
Value two stages PV power plant							400 V	353 V	20 A

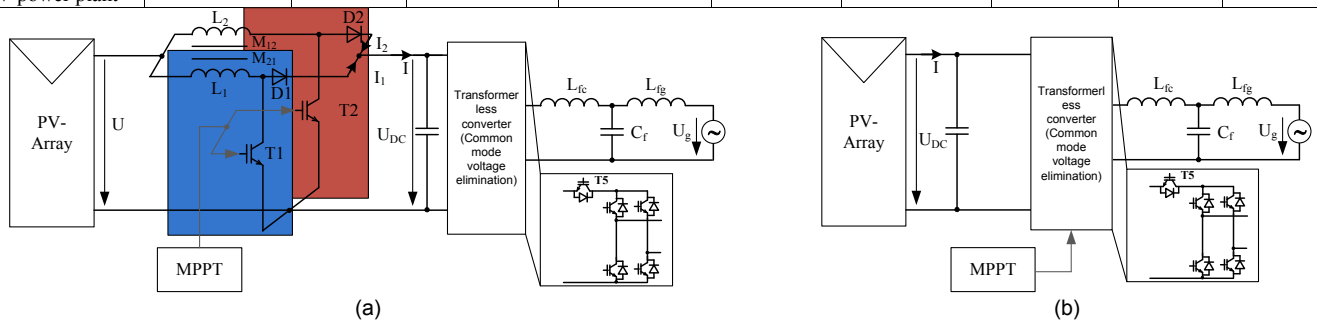

Fig. 2. Single phase grid connected PV converter: (a) with boost converter, (b) without boost converter.

to cause severe thermal stress. The optimal point of operation is changing with the irradiance and thus over the time. On days with fast passing clouds the irradiance is varying fast and thus the optimal set point for the MPPT changes, too [19]. The passing clouds cause power cycling for the power semiconductors and thus cause additional thermal cycles of the junction temperature, which reduces their lifetime.

Independently from the chosen topology, the variation of the irradiance causes thermal cycles, which is shown in Fig 3 (a) for a two stage PV power plant and in Fig. 3 (b) for a single stage PV power plant as shown in Fig. 2 with the parameters of table I. For the comparison, both plants are connected to the same PV power (P_{PV} =*5.2 kW*), but in the double stage plant, the number of parallel connected strings is higher to utilize the boost function of the converter. The irradiance is changed trapezoidal from 30% to 100% and back to 30% as done in standard test conditions. Because of the variation of the DC-link voltage in the single stage, the results can only partially be compared, but the affected thermal swing on the IGBTs is approximately $\Delta T = 55\ K$ for the two stages system and $\Delta T = 60\ K$ for the single stage system. Thus the problem of thermal cycling is relevant for both topologies: the single-stage and double stage suffer from the same problems regarding thermal stress. In the following, the analysis based on the two stages and the DC/DC control will be carried on. A similar analysis could be extended to the single-stage by modifying the grid current setpoint. However, the double stage system is taken for the analysis due to its wide application in small PV power plants, which suffer most of the fast changing irradiance due to small area the PV arrays cover.

In literature many MPPT algorithms can be found, whereby most of them can be categorized in the following basic schemes:

- Open voltage measurement or short circuit current measurement
- Curve sweeping
- Perturb & Observe (P&O) or incremental conductance

These algorithms have advantages and disadvantages with respect to tracking speed, detection of partial shading conditions or thermal stress for the power semiconductors. Concerning the thermal stress, short circuit current measurement is known to be problematic for the lifetime of the system. To overcome a disadvantage of one scheme, algorithms can be combined e.g. [3]. But not only the advantages sum up: also the disadvantages, such as thermal stress of short circuit current needs to be considered. The thermal stress of the three above mentioned MPPT algorithms can be analyzed theoretically. The measurement of the open circuit voltage ($d = 0$) or the short circuit current ($d = 1$), causes a variation of thermal stress and thus thermal cycling. Worst from the point of thermal stress is curve sweeping, because the whole curve from $d=0...1$ is passed through for the MPPT and thus minimum load and maximum load is applied every time the algorithm is run, leading to significant stress. Instead, when the P&O algorithm is operating in the MPP, only low thermal stress is expected during constant irradiance. Thus among the considered MPPT strategies, the P&O is expected to be the best from the point of thermal stress. Other algorithms behave in a similar way and avoid large power swings.

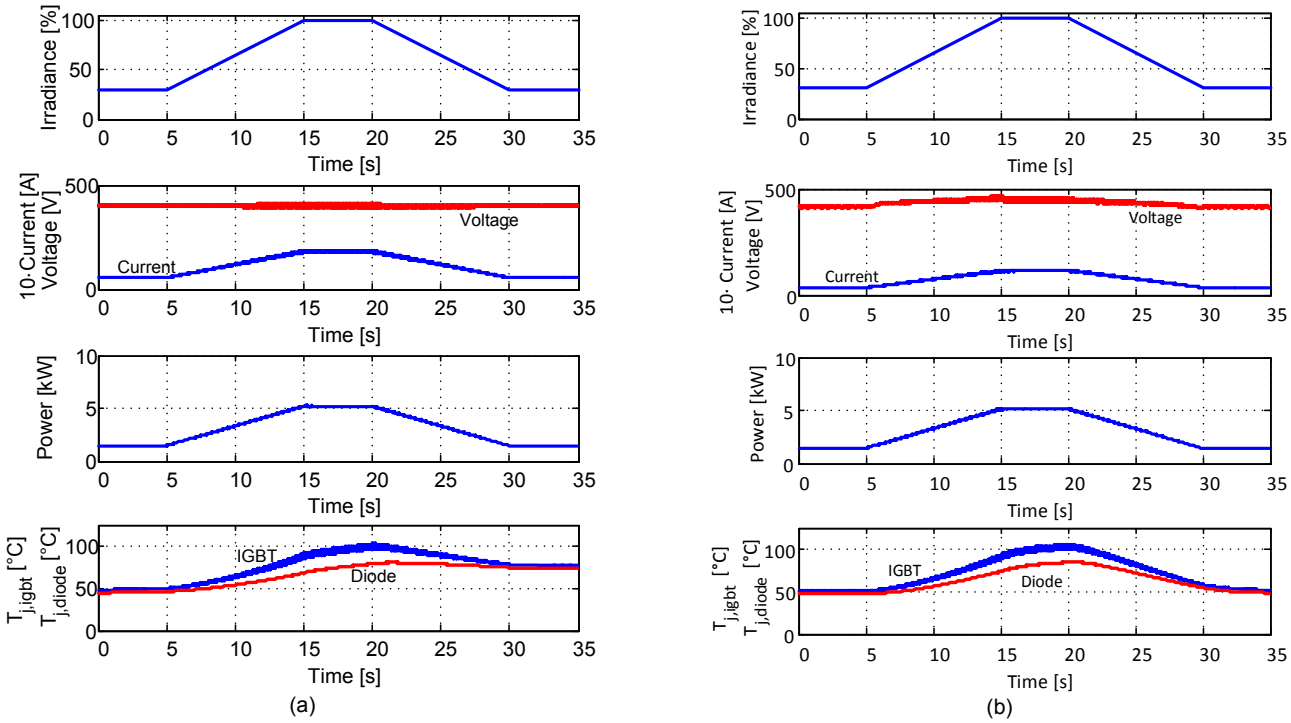

Fig. 3. Simulation of thermal stress of a single phase PV converter for a trapezoidal change of the irradiation: (a) two stages converter, (b) single stage converter.

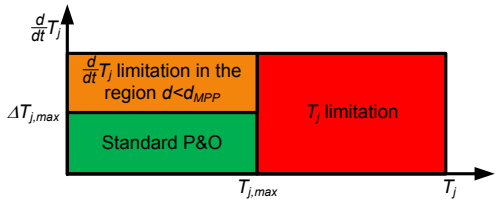

Fig. 4. Regions for application thermal stress reduction.

IV. "LIFETIME-CORRECTED" MPPT

In the following, the P&O algorithm will be used as a base for the thermal stress control due to its wide use in PV converters. In Fig. 4 the conditions are shown, in which the thermal stress reduction is applied. During fast changing radiation a positive temperature gradient limitation $\Delta T_{j,max}$ is applied and for high load operation a maximum junction temperature limitation $T_{j,max}$ is implemented. These targets can be set at the same time without conflicting with each other. The first goal to reduce thermal cycling during fast changing irradiance is implemented by limiting the positive temperature gradient at the price of a slower and less energy efficient MPPT. The gradient is chosen because of the unpredictable behavior of passing clouds, which reduce the irradiance in fast changing weather conditions. In case of a shaded PV array and dispersing clouds, it is not certain how long it takes until the next cloud shadows the array. The temperature gradient limitation shows the advantage not to influence the operation on a sunny day for an adequate temperature gradient $\Delta T_{j,max}$, but prevents excessive thermal swings during fast changing irradiance. Furthermore, in contrast to the power gradient, the junction temperature gradient addresses the cause of the failure mechanism and is not influenced by the nonlinear PV characteristics in the current source or voltage source region. This is also important for thermal cycling during varying irradiance, because the junction temperature can still cool down while the power is already increasing again. The second control target, the limitation of the maximum junction temperature $T_{j,max}$, is used to achieve maximum utilization of the power semiconductors, by guaranteeing not to excess the maximum junction temperature. This mechanism enables de-rating of the components, which reduces system costs. A flow chart shows the realization of the overall MPPT based on the P&O algorithm in Fig. 5. At the beginning of the algorithm, the electrical (U_{dc}, I_k and P_k) and thermal ($T_{j,T}$ and $T_{j,D}$) properties are sampled and updated. From the duty cycle and the dc-link voltage, the PV- array voltage can be derived as shown in (3).

The positive temperature gradient limitation is applied in region $d<d_{MPP}$ by means of a tolerance band in which the temperature can vary before the controller limits the energy harvesting. An advantage of this scheme is low influence of the noise related to the temperature measurement during normal operation. The first condition of the MPPT algorithm is to check

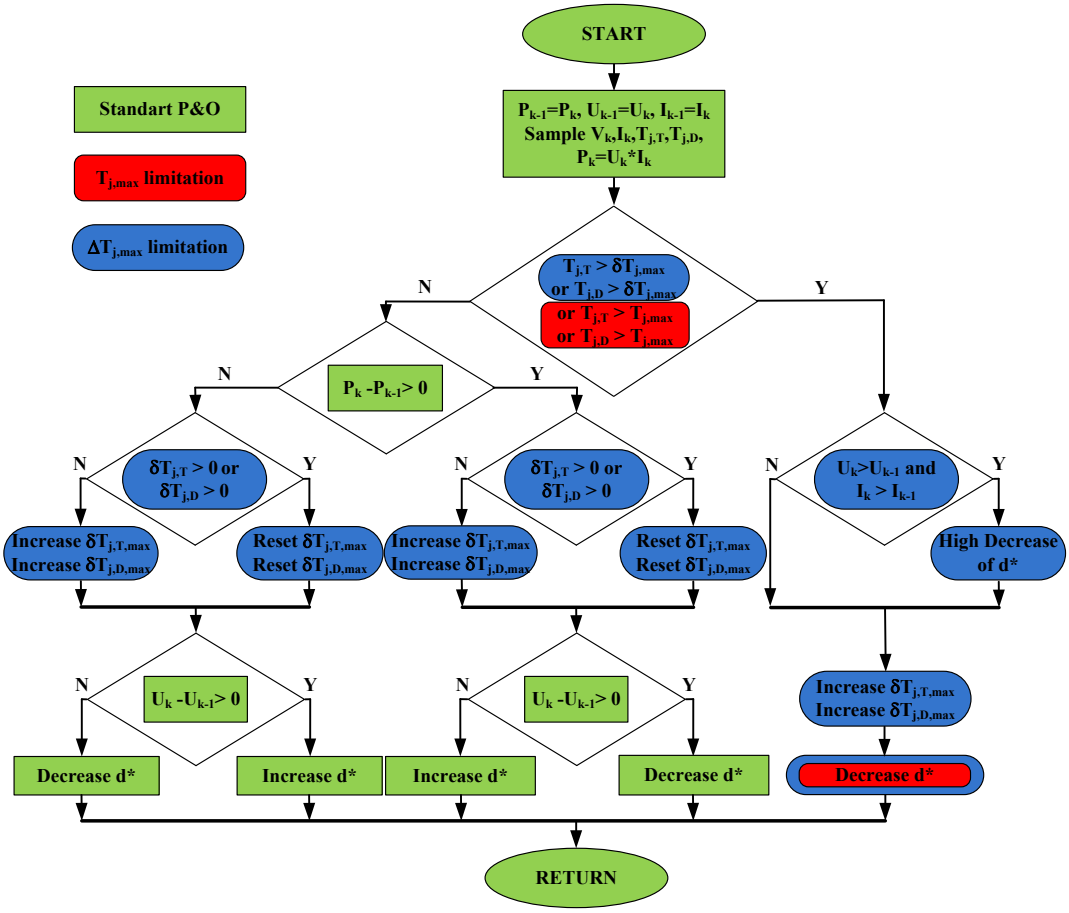

Fig. 5. Flow chart of the thermal stress and temperature limited maximum power point tracking algorithm.

the temperature limitations. In case of a violation of the maximum temperature gradient or the maximum temperature, d is increased to reduce the output power. A high increase is made in the case of power point tracking in the current source region ($d>d_{MPP}$) because of the reduced thermal stress in this region. If no temperature violation is detected, the normal P&O algorithm is carried out with the comparison of the power variation and the voltage variation. Additionally, the new thermal limitation for the next maximum temperature gradient limitation needs to be set. This part is independent from the power variation, but in the case of a temperature decrease, the new maximum temperature of the next step is set to the temperature given by the gradient limitation. Otherwise, for increasing temperatures, the new maximum temperature is the sum of the old maximum temperature and the applied gradient. In (4) the mathematical expression is shown.

$$\delta T_{j,max} = \begin{cases} T_{j,max} + \Delta T_{j,max} \cdot T_{mppt} & \frac{d}{dt} T_j(t) > 0 \\ T_j + \Delta T_{j,max} \cdot T_{mppt} & \frac{d}{dt} T_j(t) < 0 \end{cases} \quad (4)$$

V. Tuning of the Proposed MPPT Algorithm

A. Mission profiles of PV converters

The irradiation of the PV panels defines the mission profile of the PV converter and thus the thermal stress for the power semiconductors. These irradiation characteristics are influenced by the unpredictable passing clouds. Despite the uniqueness of each measured irradiance profile, the general characteristics are similar. An example of an irradiance measurement with high sampling time is presented in [20]. The irradiance in Tallinn is measured with a sampling rate of *1 s* for 2.8h. This study illustrates the frequency distribution of 150 illumination windows in cloudy conditions, whereby 2/3 are in the high irradiance region. Furthermore, out of all windows, 2/3 were shorter than 65 s and 1/3 were even shorter than 23 s. These fast varying irradiance conditions are addressed in few publications, which optimize the maximum power point tracking without taking into account the damage caused on the system. Considering this damage and cloud speeds higher than 8 m/s, even large PV power plants suffer from high thermal stress under fast changing irradiance. In Table II the time constants, which are influencing the process are shown as well as expected cloud speed to highlight the relevance of the thermal stress during fast changing irradiance. The important time constants are the maximum power point tracking speed, the varying irradiance and typical large time constants of thermal impedances (junction to case) in power electronic modules. The smallest time constant is the MPPT period, while also the thermal impedance has a relatively small time constant. However, it should be considered, that passing cloud fronts, which are shading the PV panels smooth the variation in irradiance.

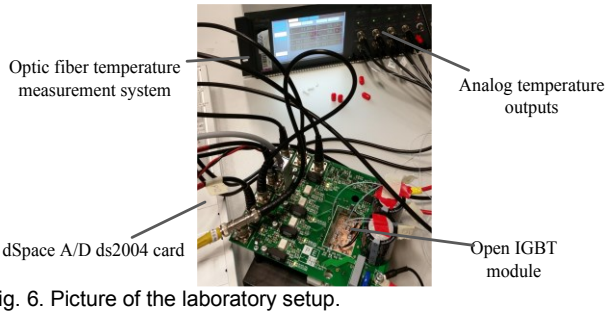

Fig. 6. Picture of the laboratory setup.

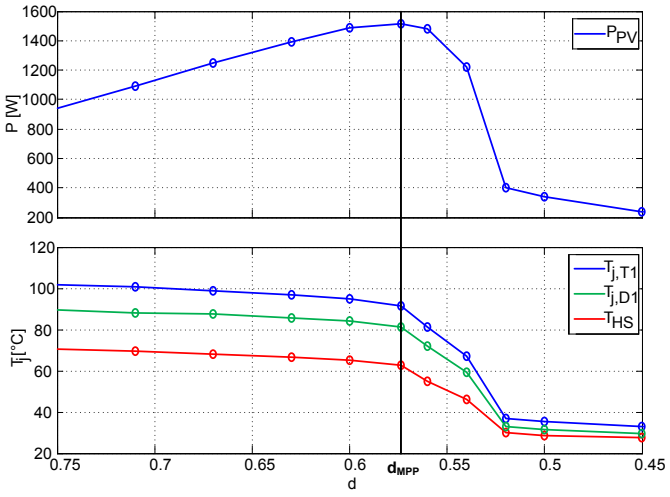

Fig. 7. Measured PV output power and junction temperature of the power semiconductors of the boost converter for varying duty cycles and constant irradiance.

To evaluate the potential of thermal stress reduction by MPPT, the described weather conditions of [20] are used to estimate how much the thermal stress can be reduced for which cost of energy. The fast changing clouds were measured in 13% of the time, which corresponds to the potential, when the MPPT algorithm can reduce the thermal stress. For the potential estimation, two different positive junction temperature gradients are considered for the algorithm. The gradients are assumed to require 23 s and 65 s respectively to the MPP. This enables to analyze best case and worst case scenarios for the reduced energy harvesting and lifetime extension during this profile. This leads to a reduction of 0.8-1.1% of the harvested energy for the higher maximum junction temperature gradient

TABLE II
TME CONSTANTS OF THE PV SYSTEM.

Property	Time constant [ms]
T_{MPPT}	50
Slowest time constants of thermal impedances of power semiconductors $Z_{th,jc}$	282
Variations in the irradiance	>1000
Time to MPP (of the applied algorithm)	~5000
Expected cloud speed	> 8 m/s

TABLE III
POTENTIAL ESTIMATION FOR THE THERMAL STRESS REDUCED MPPT IN CASE OF FAST VARYING CONDITIONS (13% OF TIME IN A YEAR).

Propsed temperature gradient limitation [K/s]	Yearly reduction of energy harvesting using the modified MPPT [%]	Stress reduction under varying irradiance [%]
0.5	[0.8 1.1]	[0, 41]
0.33	[1.6 2.8]	[33 83]

TABLE IV
SYSTEM PARAMETERS.

Variable	*Switching frequency f_s*	*Irradiation*	*U_{dc}*	*L_1=L_2=M_{12}=M_{21}*	*U_{OC}*	*I_{SC}*
Value	15 kHz	1 kW/m^2	380 V	3 mH	180 V	10 A

and 1.6-2.8% for the smaller maximum gradient. For a rough estimation about the reduced thermal stress, (2) and (3) are used with the irradiance instead of the temperature and the possible reduction in the cycles. Furthermore, the described severe thermal cycles, which can be manipulated by the MPPT are assumed to obtain similar magnitude and their time periods are equally distributed. This results in a stress reduction of up to 41.2 % for the higher maximum junction temperature gradient and up to 82.8% for the smaller gradient.

B. Stationary performance of the algorithm

To demonstrate the effectiveness of the proposed MPPT algorithm, the behavior is tested in three different conditions:

- Steady-state operation
- A step-variation in the overall maximum junction temperature
- The temperature gradient limitation for a high increase in the irradiance.

The influence of the MPPT on the thermal stress is tested on a PV system with boost inverter in continuous current conduction mode. A PV emulator is used to emulate the PV array and the boost converter is operated in interleaved mode. The system is shown in Fig. 6 with the parameters of Table I, whereby the maximum power point is set to $U_{MPP} = 160\ V$ and I_{MPP} = 9.5 A. In the boost converter a Danfoss (DP25H1200T101667-101667) open IGBT module is used and the junction temperature measurement is done with a high bandwidth optic fiber measurement system, which is directly fed back into the used dSpace 1006 system. The dc-link is controlled by an electronic load. For thermal stress analysis, the junction temperature of the IGBT T1, the Diode D1 and one spot on the passive heat sink are measured and displayed in Fig. 7 with the parameters of Table IV for a variation of the duty cycle d. The system is driven with each d until it reaches approximately steady-state conditions. This requires a substantial long time, because the heat sink needs a long time to reach thermal steady-state. Remarkably, the Maximum Power Point (MPP) with the duty cycle d_{MPP} is not the point with the maximum temperature for the power semiconductors. The thermal stress increases with an increase of the duty cycle, which can be explained with an increase of the current ripple and a decrease in the DC part, which leads to a lower root mean square value of the current. Thus the current ripple needs to be minimized in operation, which is achieved in the MPP. In general, the diode is colder than the IGBT and the temperature difference between the power semiconductors and the heat sink temperature increases with the temperature of the power semiconductors. Furthermore, the operation points with equal power transfer for $d>d_{MPP}$ are more stressing than for $d<d_{MPP}$. The heat sink temperature even reaches a 70 °C compared to 62 °C in the MPP.

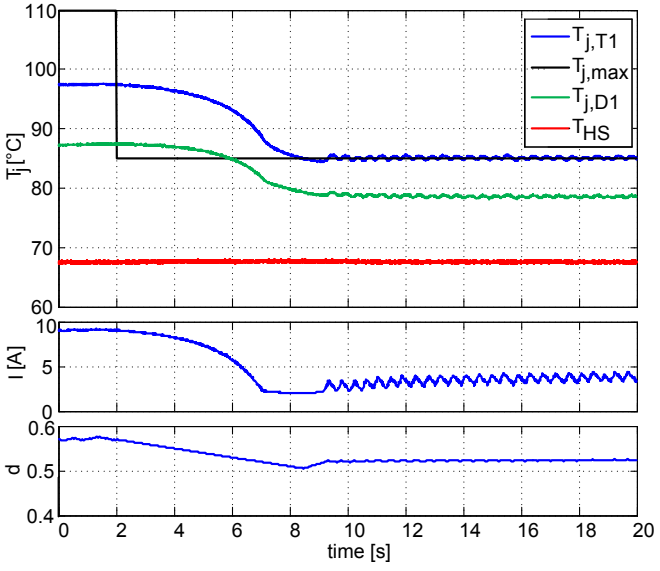

Fig. 8. Behavior of the MPPT for a step in the maximum junction temperature $T_{j,max}$ = *110 °C -> $T_{j,max}$ = 85°C* and T_{mppt} = *50 ms*.

For demonstrating the effectiveness of the maximum temperature limitation, the system is operated without thermal limitations until it reaches thermal steady-state conditions for an MPPT period $T_{MPPT} = 50\ ms$. This is shown in Fig. 8, where at $t = 2\ s$ the temperature limitation is changed from $T_{j,max} = 110\ °C$ to $T_{j,max} = 85°C$. Displayed are the junction sink temperatures of one IGBT and one Diode, the heat temperature, the array current and the duty cycle. The maximum temperature reference step forces the MPPT to decrease the duty cycle, which at the same time reduces the PV current and thus the temperature. The cooling down can be seen from *2 s* until $t = 8\ s$. Afterwards the duty cycle is increased again until the temperature limitation is violated. In steady-state this leads to

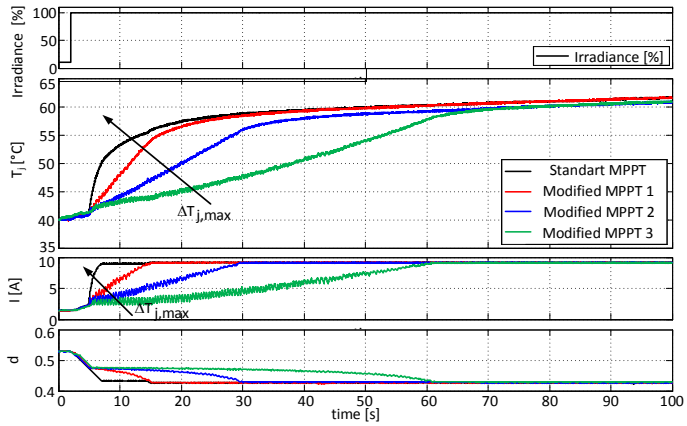

Fig. 9. Behavior of the MPPT for a step in the irradiance $P_{PV,rel}$ = *10% ->$P_{PV,rel}$ = 100%* for different temperature gradients and normalized starting temperature in one IGBT.

an oscillation of the output power and a consequent oscillation of the junction temperatures, which can be seen in the profile of the currents I. This oscillation can be reduced by either reducing the step size of the MPPT or the execution period T_{mppt}. The disadvantage is a slower tracking of the MPP, which is undesired. The diode has a lower temperature than the IGBT in the whole experiment and the temperature of the heat sink changes only marginally. Next, the junction temperature gradient limitation is tested. To achieve a sufficient increase in the temperature, the irradiance is set to $P_{PV,rel} = 10\%$ and increased in a step to $P_{PV,rel} = 100\%$. This experiment is done for standard MPPT and for $\Delta T_{j,max} = \{1, 0.5, 0.33\} K/s$. In the following $\Delta T_{j,max} = 1$ corresponds to Modified MPPT 1, $\Delta T_{j,max} = 0.5$ corresponds to Modified MPPT 2 and $\Delta T_{j,max} = 0.33$ corresponds to Modified MPPT 3. The results are shown in Fig. 9 for the junction temperature of the IGBT, which was discovered to reach the highest temperature in the boost converter.

Without the gradient limitation, the MPPT directly detects the new maximum power point after *5s*, while the temperature of the IGBT is increasing quickly. The maximum temperature gradient limitation holds in all cases and the maximum power point is reached after *13 s*, respectively *28 s* and *58 s*. Even if the most stringent temperature gradient limitation of $\Delta T_{j,max} = 0.33 K/s$ holds, the instantaneous increase of the temperature for an increase of the duty cycle is challenging the algorithm and sets the limit for the given experiment in the system, parameter tuning and measurement equipment.

VI. Lifetime Estimation of the Proposed MPPT Algorithm

To evaluate the behavior of the controller during unpredictable changes in the irradiance, a *620 s* mission profile is created and the thermal controller is tuned with the similar temperature gradients as in the previous experiment to investigate the tradeoff between reduced thermal stress and maximum power harvesting. Compared to the standard for MPPT profile testing [21], the irradiance profile is changed to have short ramp up/down times and different magnitudes and time periods to see the behavior under different conditions. Standard trapezoidal MPPT testing profiles were not used because they would lead to a repetition of the temperature profiles, while the used profile shows the response to different variations in frequency and irradiation cycles. The profile is characterized by irradiance cycles with time periods of 4 s and 50 s, which is within the time affected by the thermal controller as shown in Fig. 9 and similar junction temperature gradient limitations $\Delta T_{j,max} = \{1, 0.5, 0.33\} K/s$.

To evaluate the achieved benefits and the costs for the MPPT algorithm, an estimation of the lifetime consumption needs to be made. The mathematical model of the LESIT results is used in combination with linear damage accumulation as described in (1)-(2) and Rainflow counting is applied to identify the thermal cycles from the mission profile. The histograms with *20* boxes with a width of *1 K* for the thermal swings of all tunings are shown in Fig. 10.

The higher the magnitude of a cycle, the higher is its impact on the lifetime consumption. Without the temperature gradient limitation, the histogram shows one cycle for the magnitudes $\Delta T = \{18, 16\}$ K and 2.5 cycles with a magnitude of $\Delta T = \{12, 13\} K$. Furthermore, there is one cycle at $\Delta T = 10 K$ and 5 cycles with a magnitude $\Delta T < 5 K$. For the temperature gradient limitation with the modified MPPT 1, the high magnitudes are

remaining, but one cycle with a magnitude of $\Delta T = 13 K$ is reduced and a new cycle at $\Delta T = 8 K$ is new in the histogram. Caused by the implementation of the temperature gradient limitation in this work there are 10 cycles with a magnitude of $\Delta T < 5 K$, which means there are five new thermal cycles with low magnitude. For the more stringent temperature gradient limitation, a better reduction of the thermal cycles with high magnitude is achieved. Especially, in the case of the modified MPPT 3, a considerable shift from high magnitude thermal cycles to lower cycles is achieved.

These results are basis for the derivation of the lifetime consumption of the different profiles. The results are collected in Fig. 12, together with the derived average temperature of the different profiles and the energy harvested from the PV array. The harvested energy is derived with the measurement data of the dSpace System, which implies a certain inaccuracy of the relatively slow sampling rate compared to the dynamic of the

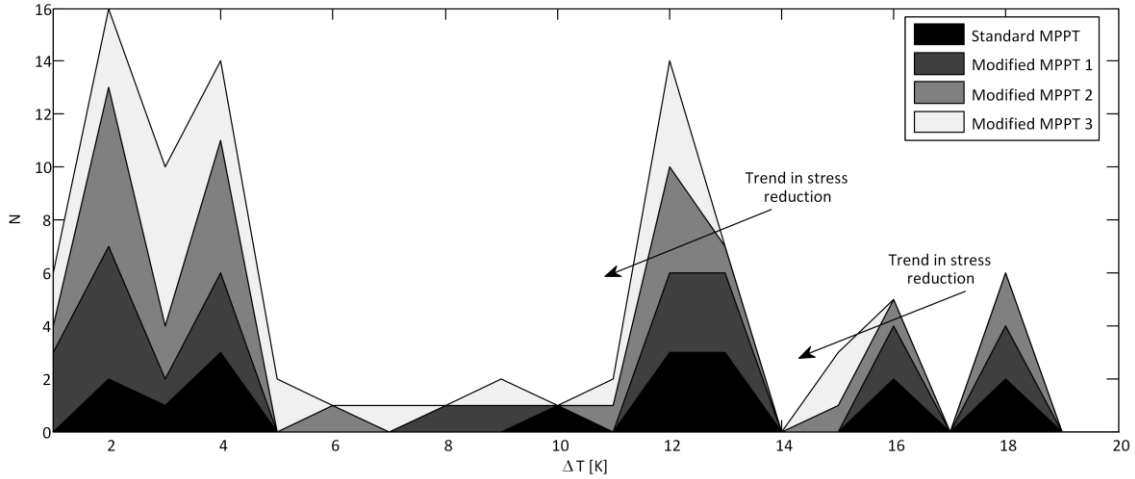

Fig. 10. Rainflow histogram of a 10 min mission profile, whereby the area represents the cycles.

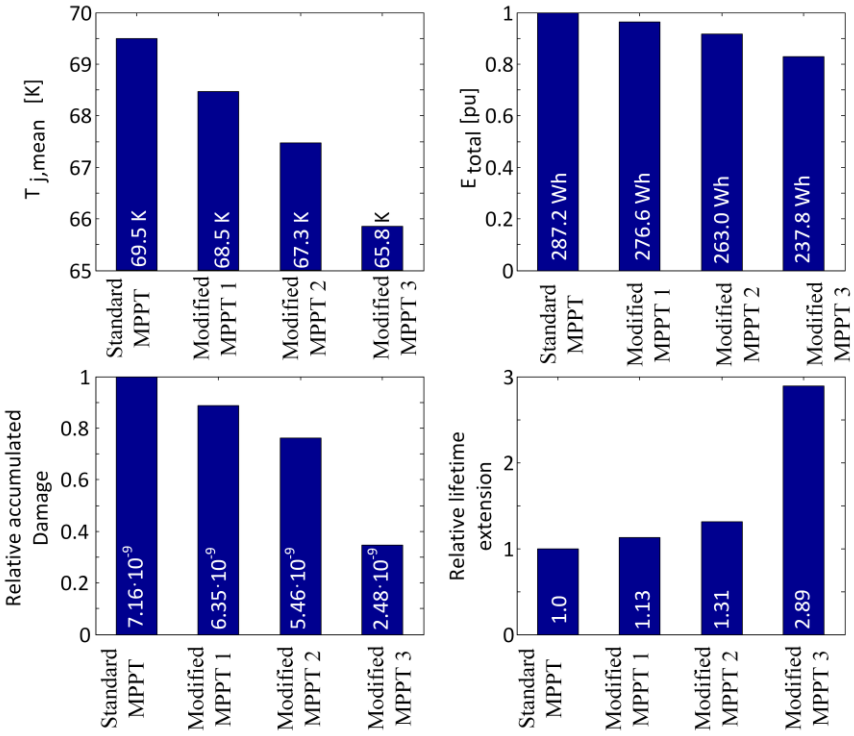

Fig. 11. Analysis of the mission profile tests with different positive temperature gradients.

currents. Similar, the thermal steady-state before the experiment is started might not be totally equal, leading to an imprecision of the average temperature. However, a limitation with the modified MPPT 1 leads to a reduced average temperature by *1 K* and only reduced energy production of *3.7 %*, while the accumulated damage is only *89 %* of the case without temperature gradient limitation. Thus under the tested mission profile, the lifetime of the system would increase by *13 %* compared to the system without temperature gradient limitation. For the more stringent limitations this trend is amplified, showing the tradeoff between maximum energy harvesting and increased lifetime. In the case of the highest temperature gradient limitation of the modified MPPT 3, the average temperature is decreased by *4.7 K* and the energy production is reduced to *82,8 %* of its possible value, while the lifetime is increased to *289 %*. Despite the reduction of the harvested energy, it must be considered that the majority of the energy harvested by a PV system comes from sunny days, while the temperature gradient limitation affects the operation only during fast-changing irradiance conditions. As a matter of fact, while the total accumulated damage is greatly reduced, the loss in harvested power may not be so relevant, if the total useful life of the system is considered.

VII. Junction Temperature Measurement or Estimation

The implementation of the algorithm requires knowledge of the junction temperature, that can be obtained with direct junction temperature measurement (e.g. with an additional diode on the chip [22]), Thermo Sensitive Electrical Parameters [23] or models and observers (e.g. [24]). The measurement solutions require additional hardware, which increases the cost. Thermal models instead, do not cause additional costs, but the precision is not guaranteed and parameter variations due to aging are a problem. However, the models can detect thermal cycles and even if the magnitude is not precise, the thermal controller can respond and reduce the thermal swing accordingly.

A deep and through discussion of the use of observers to estimate the junction temperature is out of the scope of the present paper and it is discussed in [25] but here the principle of operation of an estimator, which relies on a low bandwidth case temperature measurement, commonly integrated in today's power electronic modules, and a second order thermal model of the power module is shown. This model is fed by the derived losses of the converter and provides the junction temperature estimation. The resultant response of the thermal model on a variation in the current is shown in Fig. 12. As it can be seen, the stationary precision is not given, but the thermal swing is detected with quickly. Since this is an open loop estimation, the junction temperature estimation is not expected to result in a coupling with the controller reaction.

VIII. Conclusion

High performing MPPT algorithms, which can maximize energy harvesting also in extremely variable irradiance conditions, have been proven to lead to high thermal stress for the power electronics devices which can lead to higher failure rates. Different MPPT strategies for two stages PV power plants have been analyzed and hill climbing methods have found to cause least thermal stress for the power semiconductors. The perturb and observe algorithm has been further improved with a limitation of the junction temperature gradient of the power semiconductors to reduce the thermal stress during fast changing irradiance. For a mission profile subjected to fast changing irradiance the tradeoff between energy harvesting and

lifetime consumption is experimentally demonstrated. Reduced thermal stress and thus improved reliability of the power electronic components is achieved at the expense of reduced energy harvesting. Under tested conditions, a reduction of *3.7 %* of the energy harvested has increased the lifetime for the investigated mission profile by *13 %*.

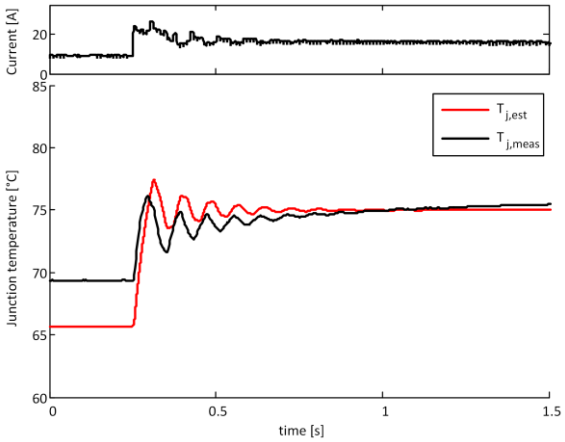

Fig. 12. Response of a junction temperature estimator on variations in the current and comparison with direct measurement.

ACKNOWLEDGEMENT

The research leading to these results has received funding from the European Research Council under the European Union's Seventh Framework Programme (FP/2007-2013) / ERC Grant Agreement n. 616344 – Heart.

REFERENCES

[1] R. Teodorescu, M. Liserre, P. Rodriguez, "Grid converters for photovoltaic and wind power systems," vol. 29, *John Wiley & Sons*, 2011.

[2] N. Femia, G. Petrone, G. Spagnuolo, M. Vitelli, "Power electronics and control techniques for maximum energy harvesting in photovoltaic systems," *CRC Press*, 2012.

[3] J.S.C.M. Raj, A.E. Jeyakumar, "A Novel Maximum Power Point Tracking Technique for Photovoltaic Module Based on Power Plane Analysis of I–U Characteristics," *IEEE Trans. Ind. Electron.*, vol.61, no.9, pp.4734-4745, Sept. 2014.

[4] S.B. Kjaer, J.K. Pedersen, F. Blaabjerg, "A review of single-phase grid-connected inverters for photovoltaic modules," *IEEE Trans. Ind. Appl.*, vol.41, no.5, pp.1292-1306, Sept.-Oct. 2005.

[5] H. Wang, F. Blaabjerg. "Reliability of Capacitors for DC-Link Applications in Power Electronic Converters—An Overview," *IEEE Trans. Ind. Appl., vol.* 50 no.5, pp.3569-3578, 2014.

[6] G. Petrone, G. Spagnuolo, R. Teodorescu, M. Veerachary, M. Vitelli, "Reliability Issues in Photovoltaic Power Processing Systems," *IEEE Trans. Ind. Electron.*, vol.55, no.7, pp.2569-2580, 2008.

[7] H. Wang, M. Liserre, F. Blaabjerg, P. de Place Rimmen, J.B. Jacobsen, T. Kvisgaard, J. Landkildehus, "Transitioning to Physics-of-Failure as a Reliability Driver in Power Electronics," IEEE Trans. Emerg. Sel. Topics Power Electron., vol.2, no.1, pp.97-114, March 2014.

[8] M. Musallam, C. Yin, C. Bailey, M. Johnson, "Mission Profile-Based Reliability Design and Real-Time Life Consumption Estimation in Power Electronics," *IEEE Trans. Ind. Electron*, vol.30, no.5, pp.2601-2613, May 2015.

[9] N. Heuck, R. Bayerer, S. Krasel, F. Otto, R. Speckels, K. Guth, "Lifetime analysis of power modules with new packaging technologies," *2015 IEEE 27th International Symposium on Power Semiconductor Devices & IC's (ISPSD)*, 2015.

[10] S. Kouro, J. Leon, D. Vinnikov, L.G. Franquelo, "Grid-Connected Photovoltaic Systems: An Overview of Recent Research and Emerging PV Converter Technology," *IEEE Ind. Electron. Mag., vol.* 9, no. 1,pp 47-61, 2015.

[11] M. Andresen, M. Liserre, G. Buticchi, "Review of active thermal and lifetime control techniques for power electronic modules," *IEEE16th European Conference on Power Electronics and Applications (EPE'14-ECCE Europe)*, pp.1-10, 2014.

[12] M. Andresen, G. Buticchi, M. Liserre, "Thermal Stress Reduced Maximum Power Point Tracking for Two Stages Photovoltaic Converters," *IEEE Energy Conversion Congress and Exposition (ECCE)*, Sept. 2015.

[13] N. Baker, M. Liserre, : Dupont, Y. Avenas,, "Improved Reliability of Power Modules: A Review of Online Junction Temperature Measurement Methods," *IEEE Ind. Electron. Mag.,* vol.8, no.3, pp.17-27, Sept. 2014.

[14] H. Oh, B. Han, P. McCluskey, C. Han, B.D. Youn, "Physics-of-Failure, Condition Monitoring, and Prognostics of Insulated Gate Bipolar Transistor Modules: A Review." *IEEE Trans. Power Electron.,* vol. 30 ,no5,pp 2413-2426, 2015.

[15] M. Held, P. Jacob, G. Nicoletti, P. Scacco, M.H. Poech, "Fast power cycling test of IGBT modules in traction application." *Proceedings of Power Electronics and Drive Systems, 1997 International Conference on*. Vol. 1. IEEE, 1997.

[16] M. Ciappa, "Selected failure mechanisms of modern power modules," *Microelectronics reliability* vol.42, no.4,pp. 653-667, 2002.

[17] M. Musallam, C.M. Johnson, "An Efficient Implementation of the Rainflow Counting Algorithm for Life Consumption Estimation," *IEEE Trans. Rel.*, vol.61, no.4, pp.978-986, Dec. 2012.

[18] D. Barater, E. Lorenzani, C. Concari, G. Franceschini, G. Buticchi, *IEEE* "Recent advances in single-phase transformerless photovoltaic inverters," *IET Renewable Power Generation* (2015).

[19] D. Sera, R. Teodorescu, J. Hantschel, M. Knoll, "Optimized Maximum Power Point Tracker for fast changing environmental conditions," *IEEE International Symposium on Industrial Electronics, ISIE*, pp.2401-2407, 2008.

[20] T. Tomson, "Fast dynamic processes of solar radiation," *Solar Energy vol.* 84 no. 2, pp. 318-323, 2010.

[21] R. Bründlinger, N. Henze, H. Hüberlin, B. Burger, A. Bergmann, F. Baumgartner, "prEN 50530–The New European Standard for Performance Characterisation of PV Inverters." *IEEE Proc.of 24th European Photovoltaic Solar Energy Conf.* 2009.

[22] T. Kajiwara, A. Yamagaguchi, Y. Hoshi, K. Sakurai, J. Gallagher, "New intelligent power multi-chips modules with junction temperature detecting function," *IEEE Industry Applications Conference, 1998. Thirty-Third IAS Annual Meeting*, pp. 1085-1090, 1998.

[23] Y. Avenas, L. Dupont, Z. Khatir, "Temperature measurement of power semiconductor devices by thermo-sensitive electrical parameters - A review," *IEEE Transactions on Power Electronics, vol.* 27, no.6 pp.: 3081-3092, 2012.

[24] M. Musallam, C.M. Johnson, "Real-Time Compact Thermal Models for Health Management of Power Electronics," *IEEE Trans. Power Electron*, vol.25, no.6, pp.1416-1425, June 2010.

[25] M. Andresen, M. Schloh, G. Buticchi, M. Liserre, "Computational Light Junction Temperature Estimator for Active Thermal Control," submitted to *IEEE Energy Conversion Congress and Exposition (ECCE)* 2016.

Markus Andresen (S'15) was born in Flensburg, Germany in 1988. He received his B.Sc and M.Sc in electrical engineering and business administration from Christian-Albrechts-University of Kiel, Kiel, Germany. Since 2013 he is working towards his Ph.D degree from the chair of power electronics at Christian-Albrechts-Unversity of Kiel, Germany.

In 2010, he was an intern in the Delta Shanghai Design Center at Delta Electronics (Shanghai) Co., Ltd., China. He is a student member of the IEEE Industrial Electronics Society. His current research interests include control of power converters and reliability in power electronics.

Giampaolo Buticchi (M'13) was born in Parma, Italy, in 1985. He received the Master's degree in Electronic Engineering in 2009 and the Ph.D. degree in Information Technologies in 2013 from the University of Parma, Italy. In 2012 he has visiting Ph.D. Student at the PEMC group of The University of Nottingham. In 2014 he was awarded with the Von Humboldt Scholarship for post-doctoral researchers. He is now working as a postdoctoral research associate at the University of Kiel, Germany. His research area is focused on power electronics for renewable energy systems, smart transformer fed micro-grids and reliability in power electronics.

Marco Liserre (S'00-M'02-SM'07-F´13) received the MSc and PhD degree in Electrical Engineering from the Bari Polytechnic, respectively in 1998 and 2002. He has been Associate Professor at Bari Polytechnic and Professor in reliable power electronics at Aalborg University (Denmark). He is currently Full Professor and he holds the Chair of Power Electronics at Christian-Albrechts-University of Kiel (Germany). He has published over 200 technical papers (more than 70 of them in international peer-reviewed journals), 4 chapters of a book and a book (Grid Converters for Photovoltaic and Wind Power Systems, ISBN-10: 0-470-05751-3 – IEEE-Wiley, second reprint, also translated in Chinese). These works have received more than 15000 citations. Marco Liserre is listed in ISI Thomson report "The world's most influential scientific minds" from 2014.

He has been awarded with an ERC Consolidator Grant for an overall budget of 2 MEuro for the project "The Highly Efficient And Reliable smart Transformer (HEART), a new Heart for the Electric Distribution System".

He is member of IAS, PELS, PES and IES. He is Associate Editor of the IEEE Transactions on Industrial Electronics, IEEE Industrial Electronics Magazine, IEEE Transactions on Industrial Informatics, where he is currently Co-Eic, IEEE Transactions on power electronics and IEEE Journal of Emerging and Selected Topics in Power Electronics. He has been Founder and Editor-in-Chief of the IEEE Industrial Electronics Magazine, Founder and the Chairman of the Technical Committee on Renewable Energy Systems, Co-Chairman of the International Symposium on Industrial Electronics (ISIE 2010), IES Vice-President responsible of the publications. He has received the IES 2009 Early Career Award, the IES 2011 Anthony J. Hornfeck Service Award, the 2014 Dr. Bimal Bose Energy Systems Award, the 2011 Industrial Electronics Magazine best paper award and the Third Prize paper award by the Industrial Power Converter Committee at ECCE 2012, 2012. He is senior member of IES AdCom. In 2013 he has been elevated to the IEEE fellow grade with the following citation "for contributions to grid connection of renewable energy systems and industrial drives".